

CHAPTER IV

RESULTS AND DISCUSSION

Oligomeric precursors, silatrane complexes are synthesized directly from inexpensive and widely available SiO_2 , triisopropanolamine and ethylene glycol. Due to their stability, long chain polysilatrane can not be synthesized by ring opening polymerization. In application, one way to form a high viscosity polysilatrane can be done using the sol-gel process, which starts from hydrolysis followed by condensation of small-molecules silatrane complexes. This study was thus focused on synthesis and characterization of silatrane complexes, sol-gel transition and pyrolysis studies under various conditions.

4.1 Synthesis and Characterization of Silatrane Complexes

4.1.1 Synthesis

Silatrane synthesis in the absence of TETA catalyst took 10 times longer than the one in the presence of TETA. Most of the products precipitated are white powders, containing 2-5 species. The characterization of the isolated products is discussed as follows.

4.1.2 Characterization

4.1.2.1 Fourier Transform Infrared Spectroscopy

Figure 4.1 shows the FTIR spectra of the silatrane complexes and SiO_2 , and *Table 4.1* lists the IR spectral band assignments.

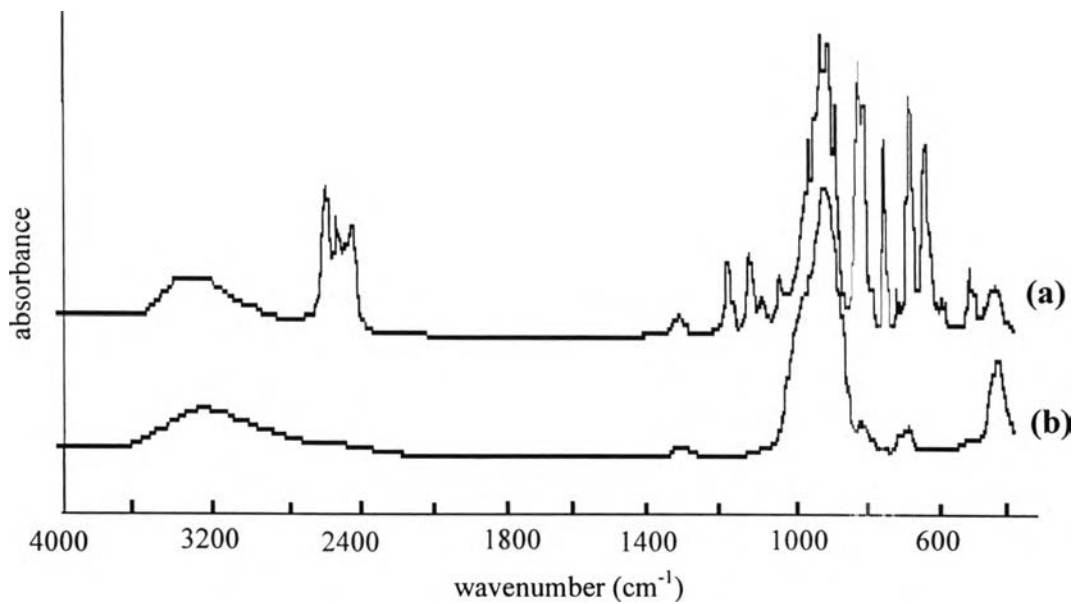


Figure 4.1 FTIR spectra of (a) silatrane complexes and (b) SiO₂.

Table 4.1 Assignments of infrared spectra of the products.

Characterization	Silatrane Complexes	SiO ₂
Si-N stretching ^a	560-590 cm ⁻¹	-
Si-O-CH ^b	970,883 cm ⁻¹	-
C-O ^a	1013-1070 cm ⁻¹	-
Si-O-CH ₂ ^b	1015-1085 cm ⁻¹	-
Si-O-Si ^b	-	1100 cm ⁻¹
C-N ^a	1270 cm ⁻¹	-
C-H bending ^a	1380-1460 cm ⁻¹	-
C-H stretching ^a	2800-29760 cm ⁻¹	-

a: Silverstein *et al.* 1991.

b: Anderson D.R., 1974.

The FTIR results show characteristic peaks of the silatrane product. The peak at 2800-2976 cm^{-1} corresponds to the C-H stretching, whereas 1380-1460 cm^{-1} results from C-H bending. The peak at 1270 cm^{-1} is assigned to $\nu\text{C-N}$. The strong peak at 1030-1070 cm^{-1} corresponds to the $\nu\text{C-O}$ and the peak at 560-590 cm^{-1} refers to the Si-N dative bond. Since the complexes contain many different molecular weights and FTIR is the method used to characterize the functional groups of the products, other structural characterizations methods are needed to distinguish different species.

4.1.2.2 Nuclear Magnetic Resonance Spectroscopy

The ^1H - and ^{13}C -NMR spectra were used to confirm the structure of silatrane complexes. ^1H -NMR spectrum of the silatrane complexes shows chemical shifts at 1.2, 2.9, 3.3, 5.7, and 4.0 ppm, which refer to CH-CH_3 , N-CH_2 , $\text{CH}_2\text{-O}$, R-OH , and CH-CH_3 , respectively. Confirmed with ^{13}C -NMR spectrum shows peaks at 20.5, 23, 57.7, 59.2, and 62.78 ppm, which are assigned to $\text{H}_2\text{C-CH-CH}_3$, $\text{H}_2\text{C-CH-CH}_3$, N-CH_2 , $\text{CH}_2\text{-O}$, CH_2OH , respectively. From these techniques the products were confirmed that they are silatrane complexes composed of several different species *Figures 4.2 and 4.3 show*, respectively, ^{13}C and ^1H NMR spectra, and the corresponding spectral assignments are presented in *Table 4.2*.

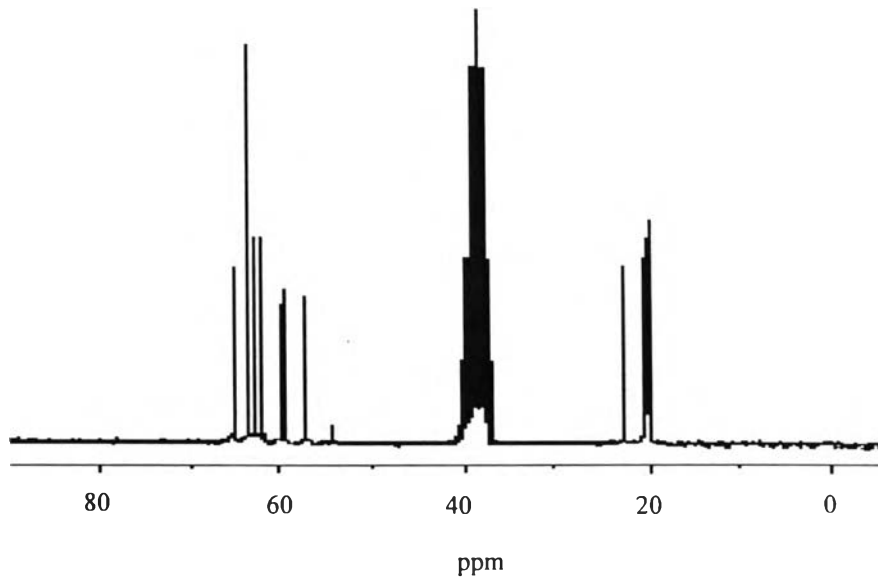


Figure 4.2 ^{13}C -NMR spectrum of silatrane products.

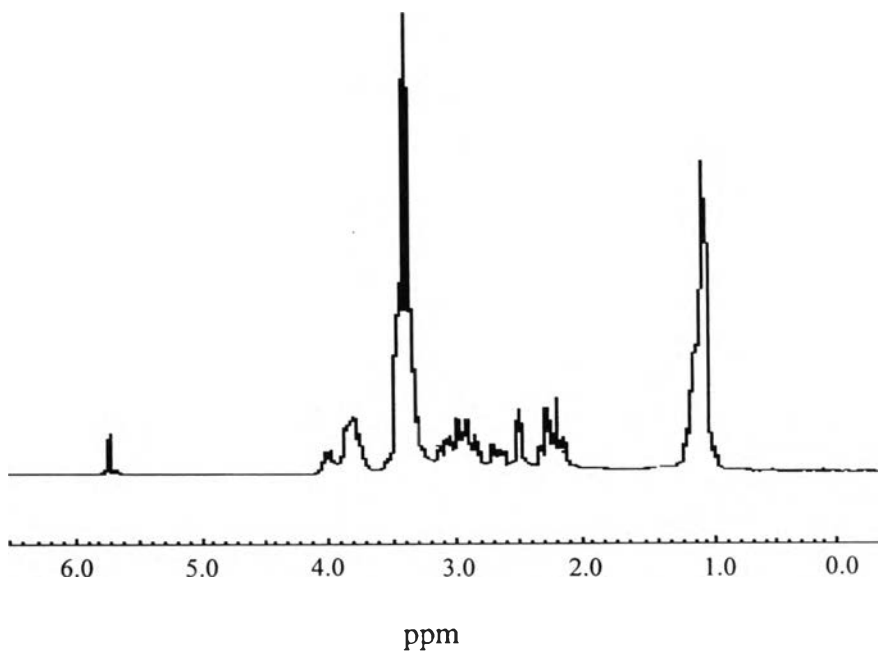
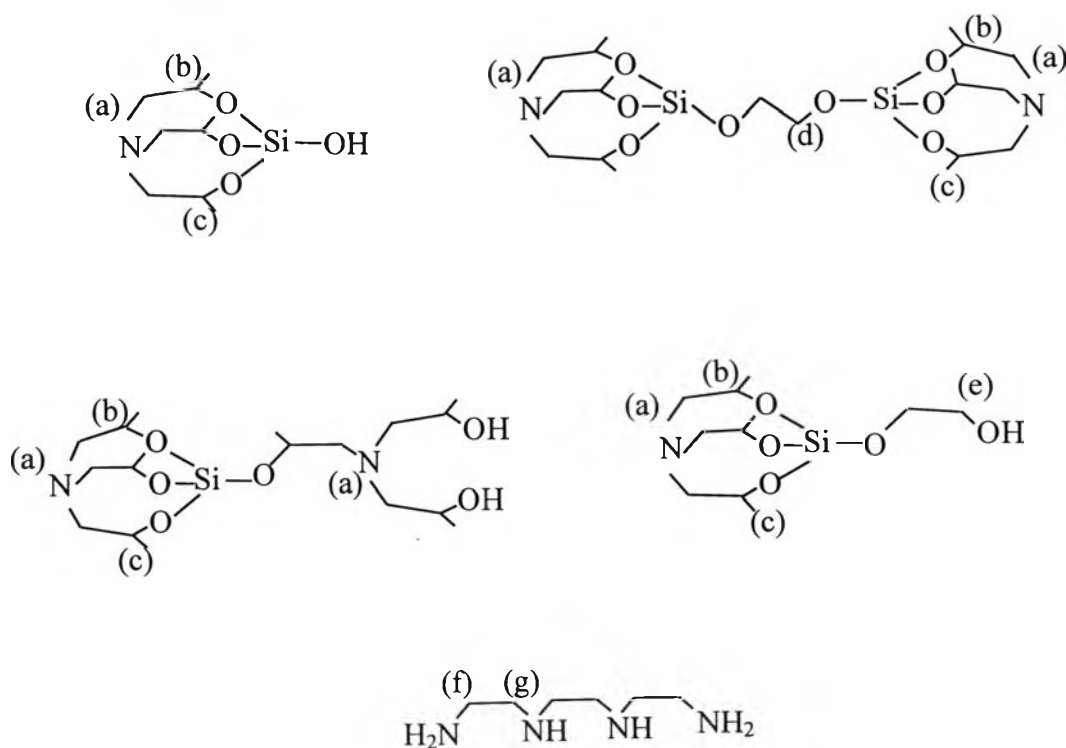


Figure 4.3 ^1H -NMR spectrum of silatrane products.

Table 4.2 ^1H - and ^{13}C -NMR chemical shifts of silatrane complexes
(Silverstein *et. al*, 1991; Piboonchaisit p., 1995).

Position	Groups	^1H -NMR (ppm)	^{13}C -NMR (ppm)
(a)	N-CH ₂	2.86-2.91	57.7
(b)	CH-CH ₃	4.0	23
(c)	CH-CH ₃	0.96-1.12	20-21
(d)	CH ₂ -O	3.3	59.2
(e)	R-OH	3.4-3.5	62.5-65
(f)	NH ₂ -CH ₂ of TETA	2.6-2.7	39-41
(g)	NH-CH ₂ of TETA	2.9-3.1	60.4-60.7



4.1.2.3 Gel Permeation Chromatography

1) Variation of Vacuum Distillation Time

Figure 4.4 shows the silatrane complex products with different molecular weight obtained from using excess TIS and varying the vacuum distillation time.

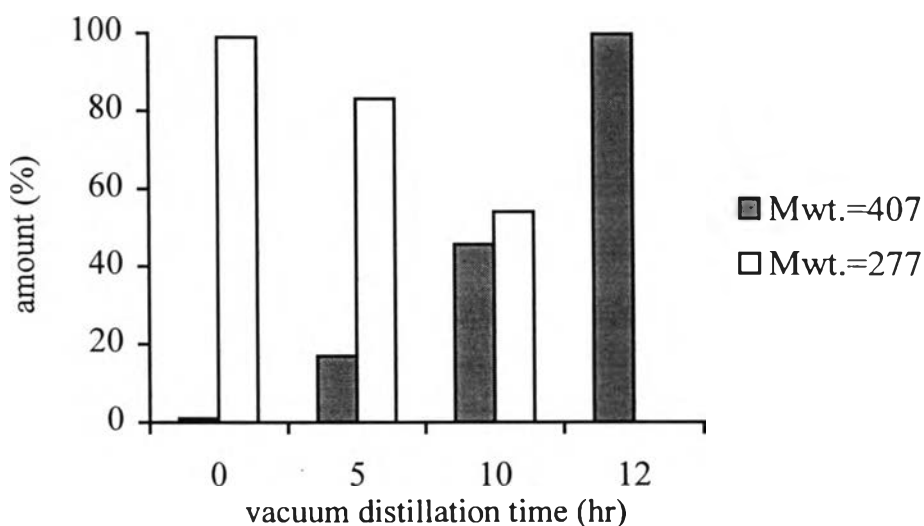


Figure 4.4 Molecular weight determination of silatrane complexes at $[\text{TIS}]:[\text{SiO}_2] = 2.5:1$, and various vacuum distillation time.

From the GPC determination, when excess TIS is used, silatranes with 2 different molecular weight, 277 and 407, are obtained. The proposed structures of products are showed in Figure 4.5.

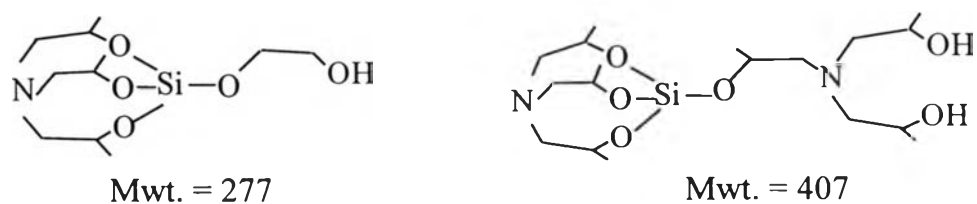


Figure 4.5 The proposed structures of silatrane complexes obtained under conditions of excess TIS.

When the reaction is completed, before removal of the residual EG under vacuum, most of the product obtained is the monomer with molecular weight equal to 277. After vacuum distillation, however, the larger species with molecular weight about 407 increases with the vacuum distillation time. The low molecular weight monomer is totally converted to the larger species with the molecular weight of 407, in 12 hr. This larger molecule (407) contains only 1 mol of SiO_2 and 2 mol of TIS, having low %silicon content, which means low % ceramic yields. The other reason is the higher consumption of TIS that will increase the cost of product. It is thus not suitable for ceramic precursors, which required low shrinkage.

2) Variation of Vacuum Distillation Temperature

When the ratio of reactants used is set at 1:1, the product structure and % ceramic yield obtained are different, especially when the vacuum distillation temperature is varied.

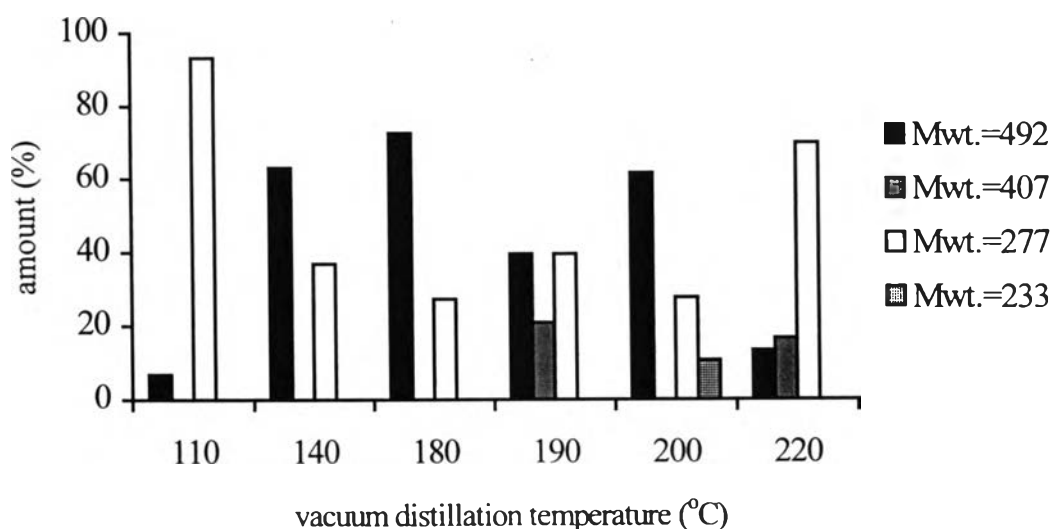


Figure 4.6 Silatrane complexes obtained at 1:1 [TIS]:[SiO_2] and various vacuum distillation temperature.

The results from *Figure 4.6* indicate 4 different possible silatrane complexes. The proposed structures are showed in *Figure 4.7*.

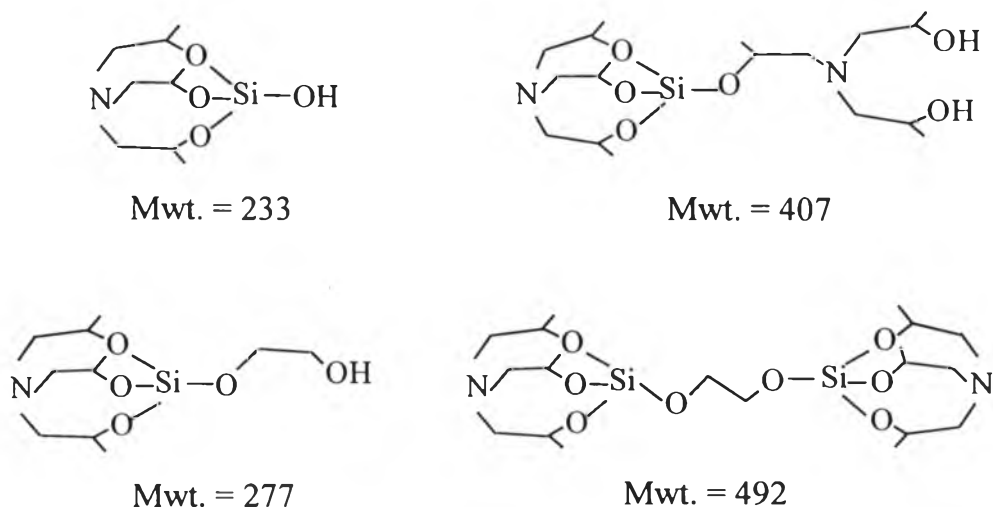


Figure 4.7 The proposed structures of silatrane complexes using 1:1 ratio of [TIS]: [SiO₂].

By using one equivalent mol of TIS the % ceramic yield of silatrane product is higher than the one with excess TIS. The molecular weight and molecular structure are also affected by vacuum distillation temperature. At low temperature, the major product obtained is the product with the molecular weight of 277. When the temperature increases, the larger molecule (492) is also increased. However, when the temperature employed is higher than 180°C, the smaller molecules again predominate which may result from a reversible reaction.

4.2 Sol-Gel Transition of Polysilatrane

4.2.1 Rheometric Measurement

Figure 4.8 shows the plot between $\tan\delta$ vs. gelling time at multi-frequency. In the sol state, $\tan\delta$ is frequency-dependent, and decreases as the gelling time increases. At the gel point, $\tan\delta$ becomes frequency independent. (The gel point is determined as the point at which the value of $\tan\delta$ becomes independent of frequency)

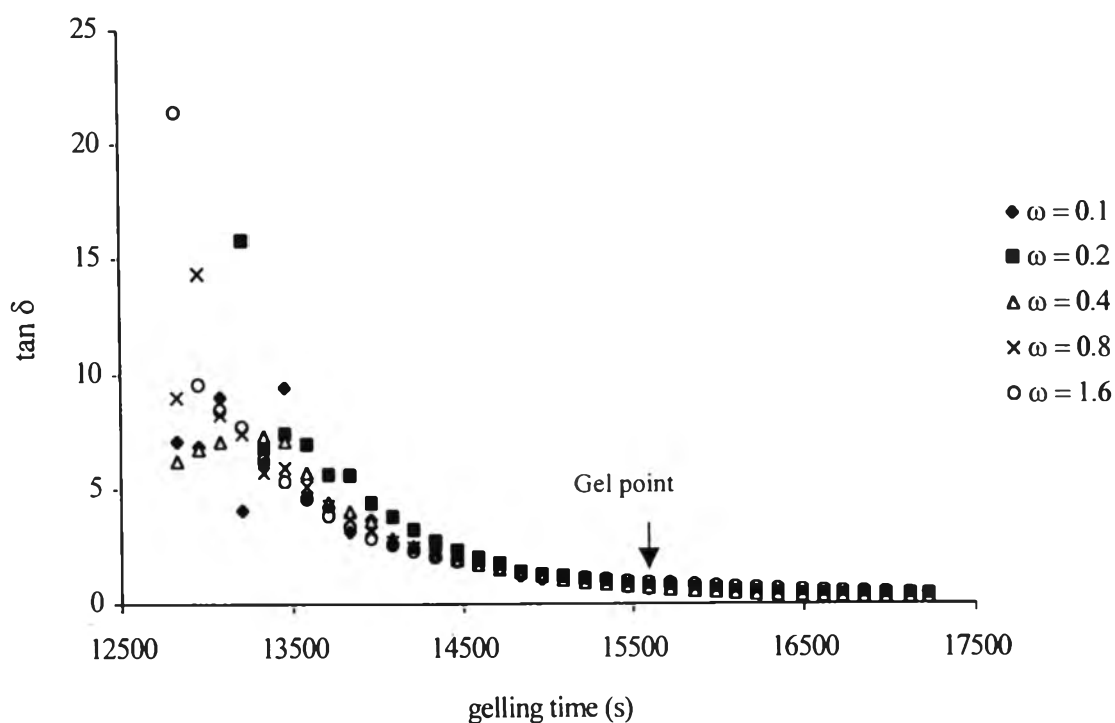


Figure 4.8 Multi-frequency plot of $\tan\delta$ vs. gelling time of 150% w/v silatrane complex hydrolyzed in water at $T = 40^\circ\text{C}$.

At the gel point, a unique power-law exponent is found from linear regression of log-log G' and G'' vs. frequency, ($n'=n''$), as shown in *Figure 4.9*.

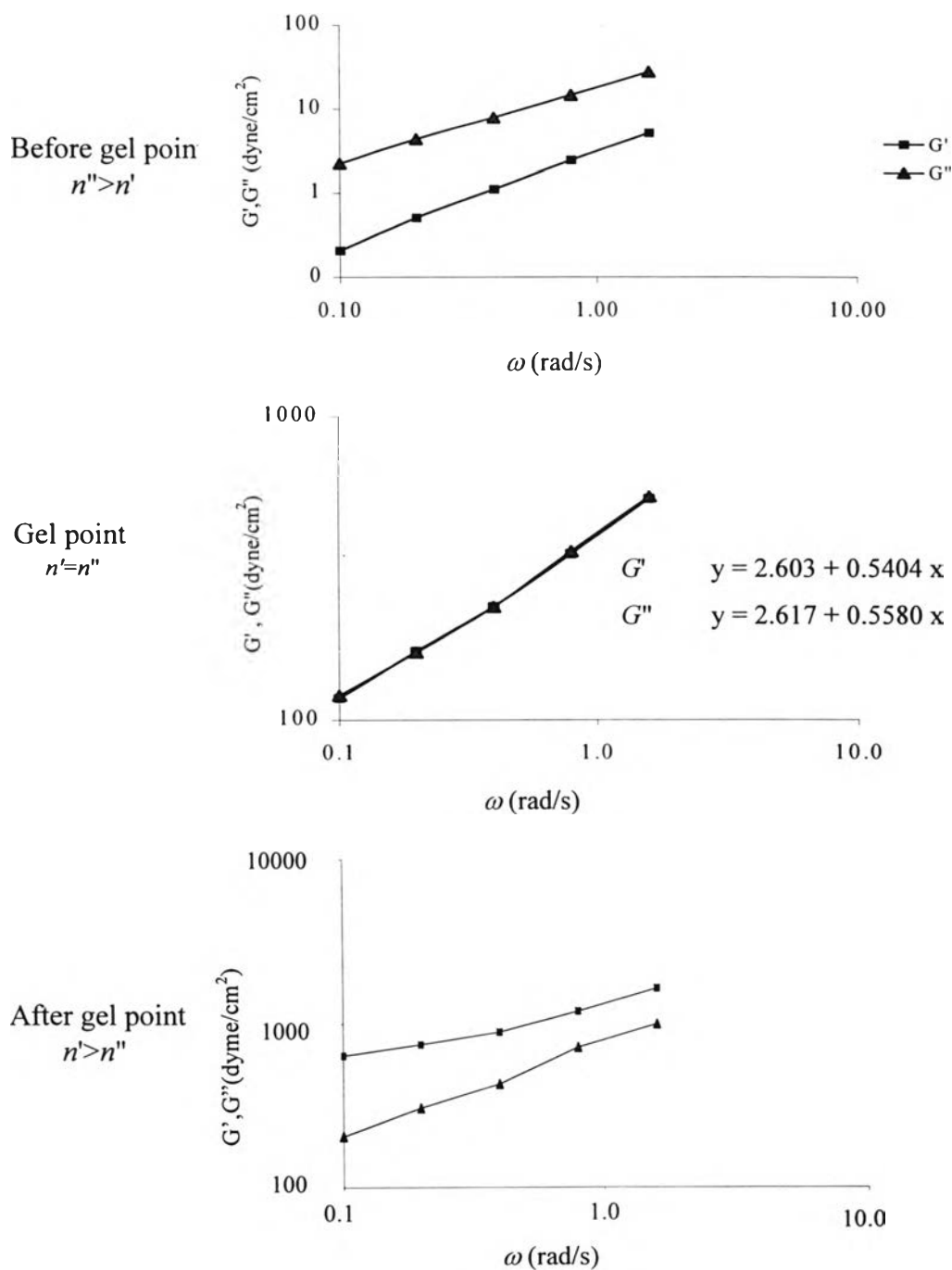


Figure 4.9 The relationship of log G' and log G'' vs. log frequency of 150% w/v silatrane complex hydrolyzed in water at $T = 40^\circ\text{C}$.

At sol state, $\log G''$ is higher than $\log G'$, meaning that the sample exhibits liquid behavior, and the slopes of $\log G'$ and $\log G''$ are not equal. When the gelation occurs, both slopes are nearly equal, as illustrated in eq. (4.1) and (4.2).

$$\text{Log } G' \quad y = 2.603 + 0.5404 x \quad (4.1)$$

$$\text{Log } G'' \quad y = 2.617 + 0.5580 x \quad (4.2)$$

After the gel point, $\log G'$ is higher than $\log G''$, indicative of a predominantly elastic behavior. Here, the power law exponents are not equal. To clarify the gel point determination, the power law exponents n' and n'' are plotted vs. gelling time, see *Figure 4.10*.

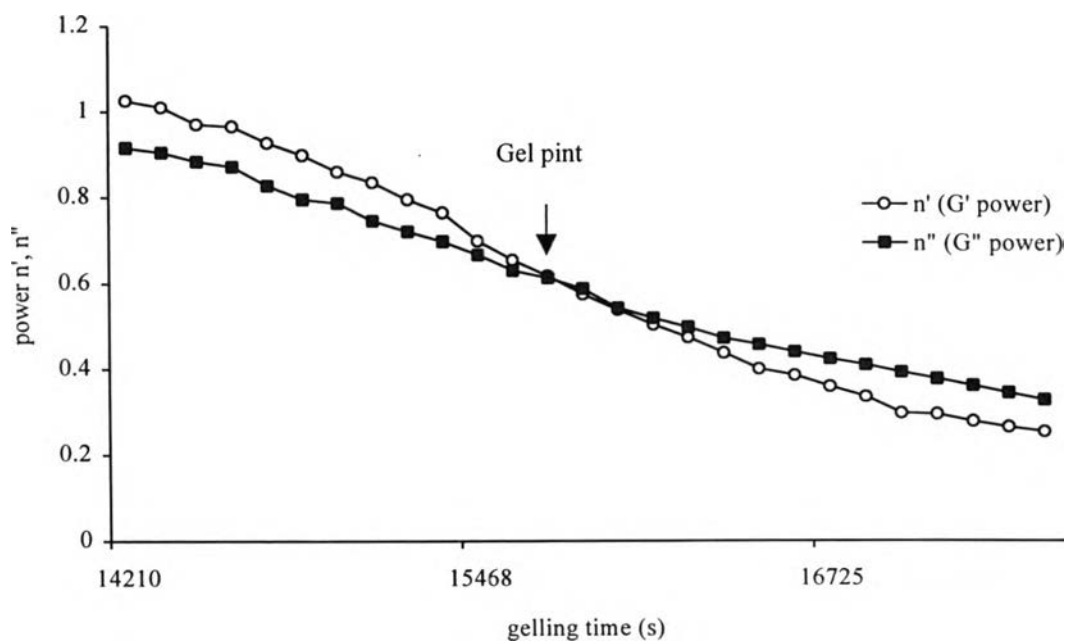


Figure 4.10 The plot of power-law exponent n' and n'' vs. gelling time of 150% w/v silatrane complex hydrolyzed in water at $T = 40^\circ\text{C}$.

Before gelation occurs, exponent n' is higher than exponent n'' . The gelling time can be estimated clearly as the point at which the exponents n' and n'' crossover $n' = n'' = 0.56$. The exponent n'' is then higher than the exponent n' after the gel point.

Figure 4.11 shows the relationship between the complex viscosity (η^*) obtained from multi-frequency scan vs. gelling time. Before the gel point, the system exhibits liquid like behavior, causing η^* to be very low. After the gel point, η^* increases rapidly, and shows a strong dependence.

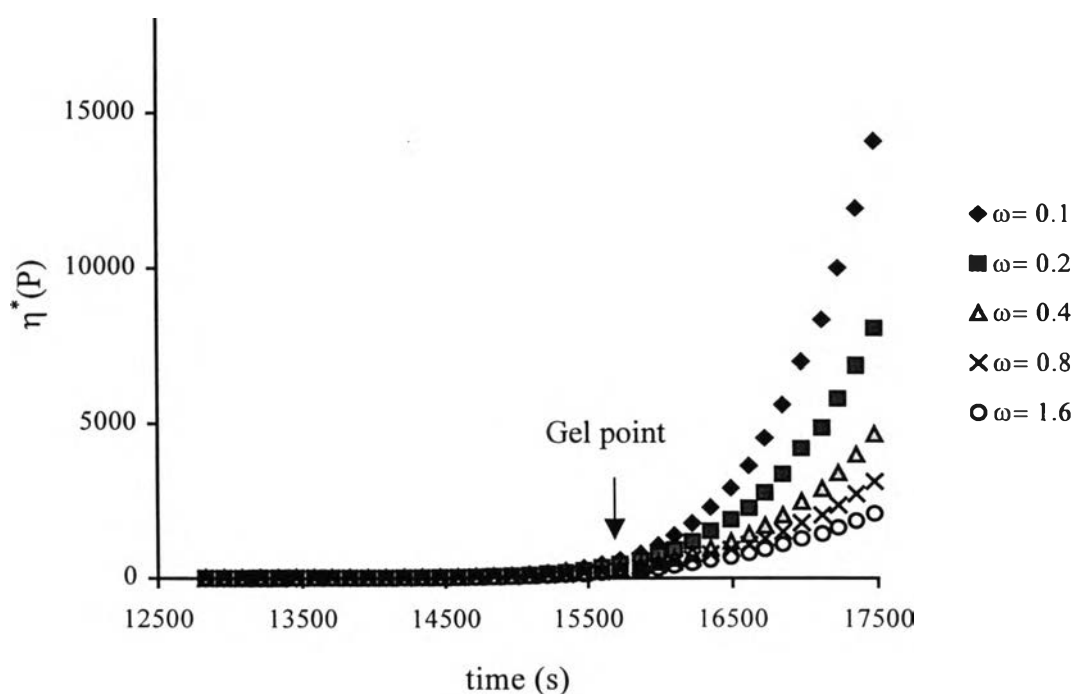


Figure 4.11 Complex viscosity (η^*) at different frequency plotted vs. gelling time of 150% w/v silatrane complex hydrolyzed in water at $T = 40^\circ\text{C}$.

To determine the gelation time, all samples are carried out by the same methods, which are quite accurate. The summary of the results for gelling time, $\tan\delta$ and the power-law exponent, n , is showed in Table 4.3.

Table 4.3 Viscoelastic properties at the sol-gel transition of polysilatrane.

Solvent	Temperature(°C)	Gelling time(s)	$\tan \delta$	n
MgO + H ₂ O	60	4702	1.44	0.65
H ₂ O	60	6410	1.83	0.79
MeOH + H ₂ O	60	8258	1.20	0.60
MgO + H ₂ O	50	8950	3.02	0.85
H ₂ O	50	10050	1.42	0.67
MeOH + H ₂ O	50	10950	1.36	0.61
MgO + H ₂ O	40	14062	1.20	0.62
H ₂ O	40	15590	1.60	0.68
MeOH + H ₂ O	40	19007	1.27	0.61

As observed from the table with presence of MgO in the solution which gives high pH (~11.3), accelerates the hydrolysis rate, resulting in the faster gelling time. On the other hand, the system that uses MeOH containing H₂O as a solvent requires longer time to gel. This means that the solution containing MeOH slows down the hydrolysis and gelation. It can be concluded that the gelling time is affected by the rate of hydrolysis. Moreover the temperature is another factor that affects the hydrolysis rate and increase of temperature accelerates the gelling rate.

In addition, it was experimentally found that increasing the gelling time or cross-linking density led to a reduction of exponent n . Under all conditions, most of the n values fall between 0.60-0.68 (0.64 ± 0.04), except conditions that using H₂O as a solvent at 60°C and MgO/H₂O at 50°C which have n values of 0.79 and 0.85, respectively. The latter two values appear to be outliers, and therefore reflect experimental error (e.g. solvent evaporation or sample loading error) which will have to be further evaluated. The experimental

range of n values is comparable to the value predicted theoretically, $n = 0.667$, if the sol-to-gel transition occurs through a percolation mechanism.

4.2.2 Fourier Transform Infrared Spectroscopy

The polysilatrane gel obtained from the above method was characterized by FTIR. *Figure 4.12* shows FTIR spectra of a polysilatrane gel compared with a silatrane complex monomer.

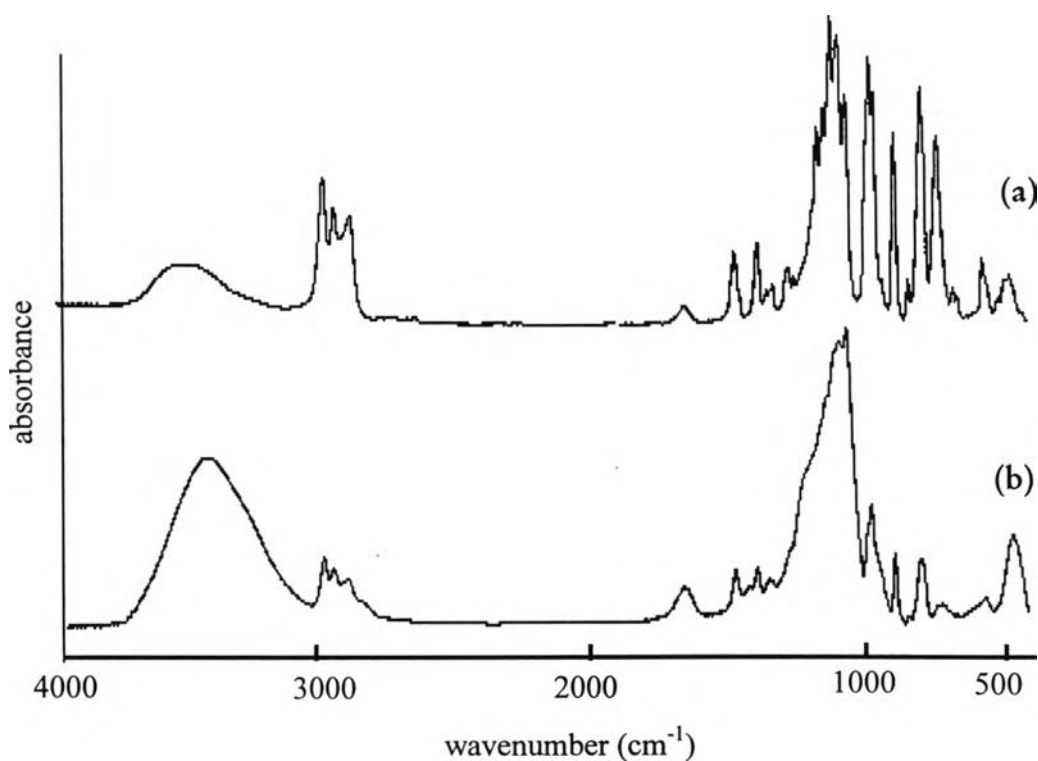


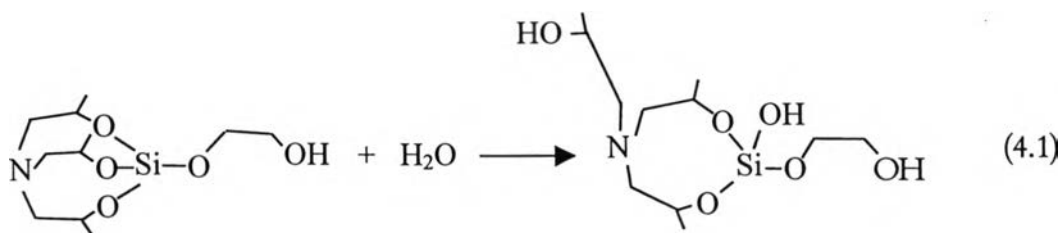
Figure 4.12 FTIR spectra of (a) silatrane complexes and (b) polysilatrane gel.

From FTIR spectra, the polysilatrane gel gives higher absorbance for OH stretching and lower absorbance of organic peaks. However it still had a peak at 560 cm^{-1} that is assigned to Si-N transannular bonding. From these results it can be concluded that the polysilatrane gel is not completely hydrolyzed to form cross-linked SiO_2 . Some of the polysilatrane chains still

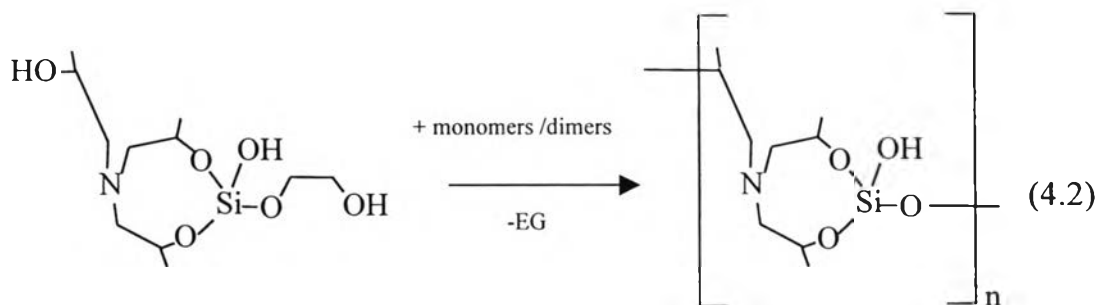
remain in the network, which can be pyrolyzed at temperature, lower than 800°C.

The residual polysilatrane chains or degree of cross-linking have an effect on the processing of ceramic precursor. At low % cross-linking, the gel exhibits low elasticity (small $\tan\delta$) and becomes more solid-like as the degree of cross-linking increase. For ceramic precursor, there are many different processing steps to the application of the final product. The optimum degree of cross-linking is therefore different for each step.

The hydrolysis and condensation reactions occurring in polysilatrane are similar to the other reactions of sol-gel processing that is described previously in the chapter II. Since, the silatrane complexes can be hydrolyzed at many positions, there are many types of mechanisms that can occur. From the FTIR results, a proposed mechanism is shown below.



The reaction (4.1) is partial hydrolysis of silatrane complex to obtain more reactive monomer. The reactive monomer is then condensed with another monomer or dimer or oligomer to obtain colloid-like oligomers, as shown in eq. (4.2).



The larger molecules will form by further hydrolysis and condensation to obtain polysilatrane. Finally the polysilatrane gel will be formed, as showed in *Figure 4.13*.

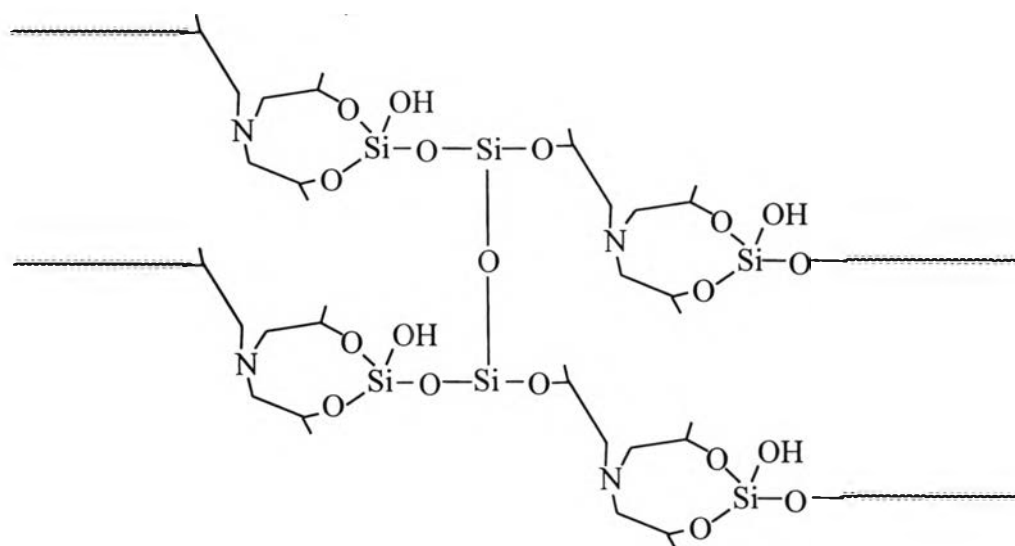


Figure 4.13 Proposed structure of polysilatrane gel.

The hydrolysis and condensation occur and result in larger molecules until high enough viscosity is obtained to be processed. After gelation has occurred, the reaction continues since the cross-linking is not yet complete in this step, leaving some organic ligand. The pure SiO_2 network is obtained by pyrolyzing the gel to 800°C to remove all organic ligands.

4.3 Pyrolysis of Polysilatrane Gel

4.3.1 Fourier Transform Infrared Spectroscopy

The gels obtained are pyrolyzed at various pyrolysis temperatures and the structures are studied using FTIR. *Figure 4.14* shows the FTIR spectra of pyrolyzed products at different temperatures.

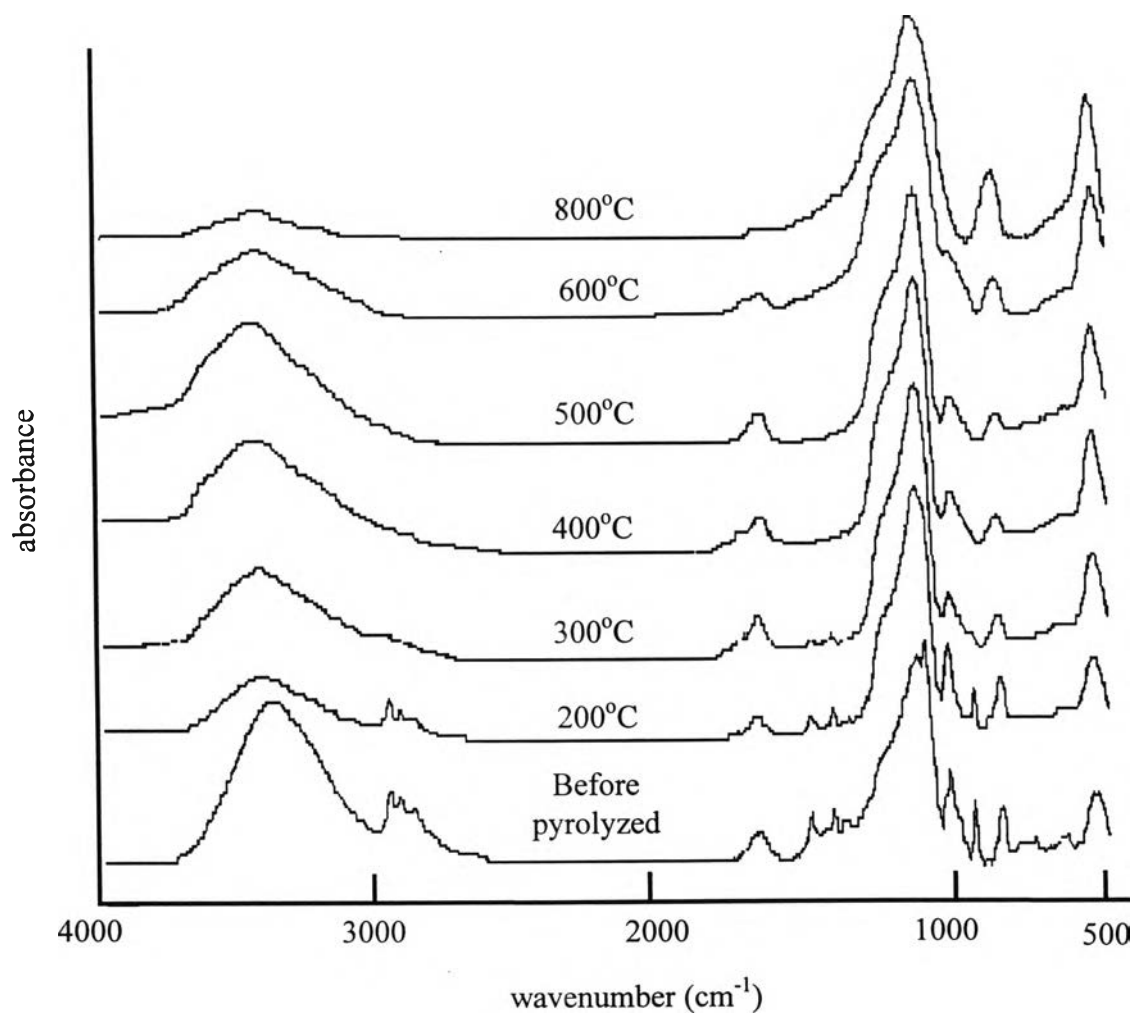


Figure 4.14 FTIR spectra of the pyrolyzed polysilatrane gel at different temperatures.

From the FTIR spectra, as the pyrolysis temperature increases, the peaks referring to organic material and a peak at 560 cm^{-1} that is assigned to the Si-N dative bond are decreased, while the peak of SiO_2 at 1100 cm^{-1} is increased. At 800°C there is only the characteristic peak of SiO_2 . That means in this precursor, the ceramic product can be obtained using processing temperature as low as 800°C .

4.3.2 BET Surface Area Measurement

The gel obtained by hydrolysis followed by condensation of silatrane complexes is studied the pyrolysis. In this section, the effects of gelling rate and pyrolysis condition are studied by BET technique and the surface area of SiO_2 product is shown in *Table 4.4*.

Table 4.4 Surface area of polysilatrane gel pyrolyzed at 800°C .

Gel	Surface area (m^2/g)
Hydrolyzed $\text{MgO} + \text{H}_2\text{O}$	417
Hydrolyzed H_2O	401
Hydrolyzed $\text{MeOH} + \text{H}_2\text{O}$	313
Pyrolyzed start from 500°C	414
Pyrolyzed start from room temp.	388

The sample hydrolyzed by MeOH , which has lowest gelling rate gives the lowest surface area, while the sample hydrolyzed by MgO solution has the highest surface area. At high gelling rate, it is likely that small gel particles are formed, leading to smaller pore sizes and a higher surface area in the pyrolysed glass. From the results, we can summarize that the gelling rate obviously has effect on the surface area. With the same reason, the sample that is started to pyrolyze at 500°C gives higher surface area than the one that started at room

started at room temperature. The remaining EG that used as solvent is decomposed rapidly at 500°C leaving high porosity in the sample.

4.3.3 Microstructure Study of Pyrolyzed Polysilatrane Gel

The microstructures of the pyrolysed polysilatrane were studied by SEM. *Figure 4.15* illustrates the different surface of pyrolyzed samples that are hydrolyzed by various solvents.

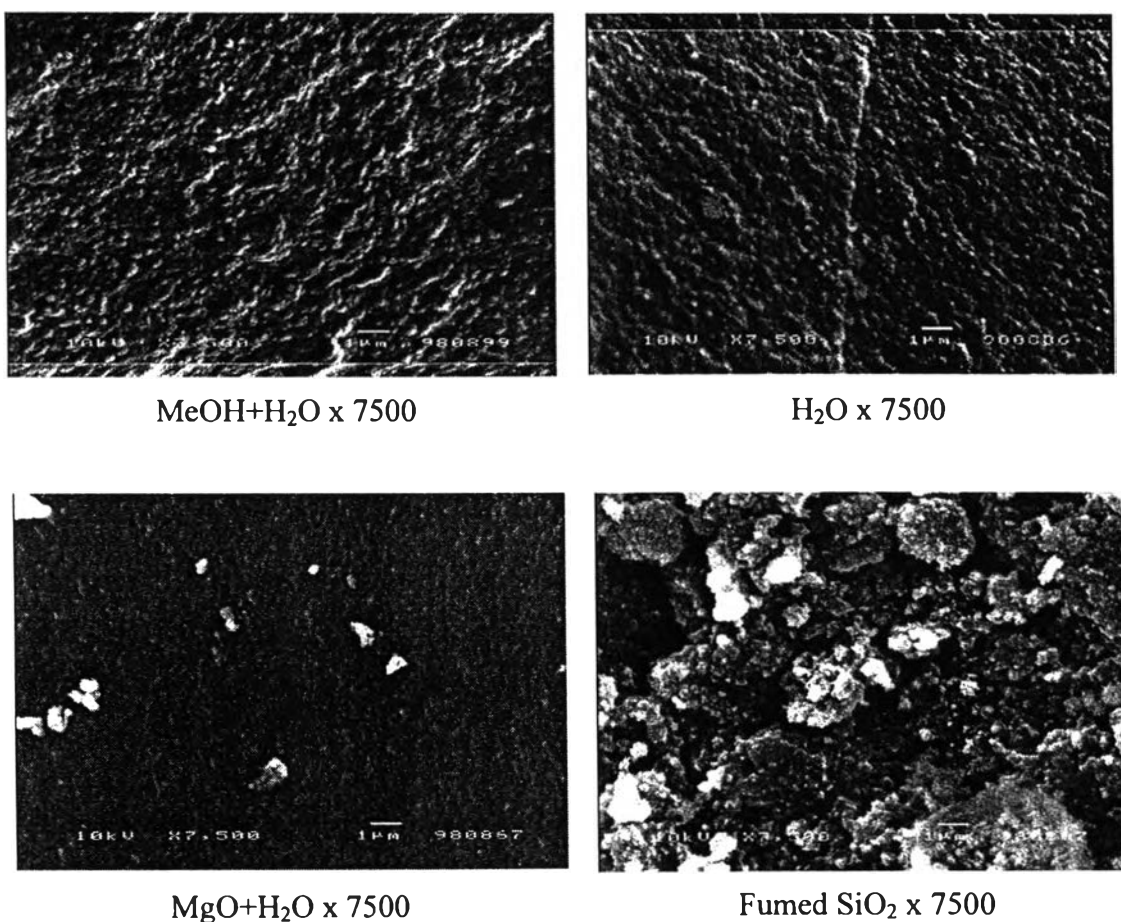
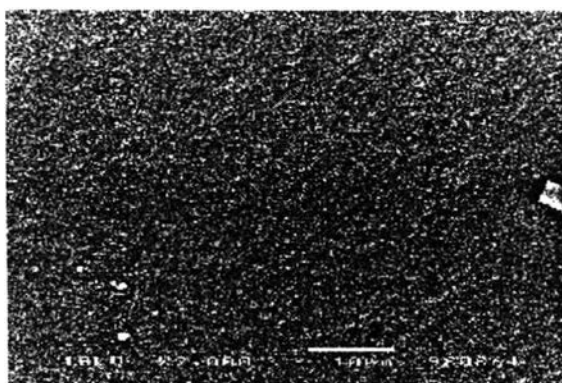
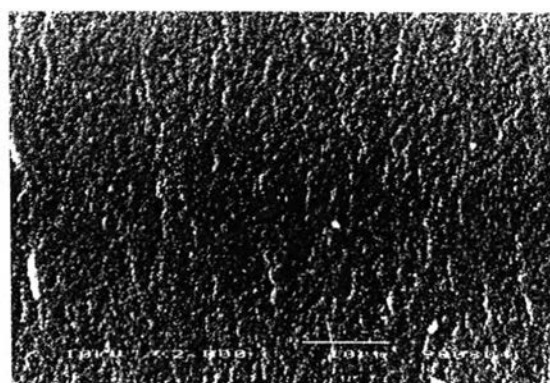


Figure 4.15 SEM micrographs of pyrolyzed polysilatrane hydrolyzed with various solvents, at 800°C, and heating rate of 10°C/min as compared with fumed SiO₂ with magnification of 7500.

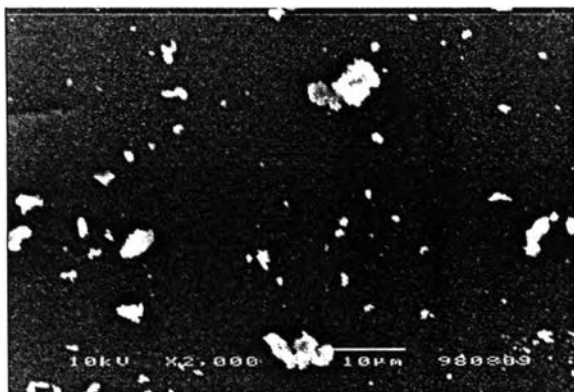
From SEM results with magnification of 7500, the surfaces are rough and have homogeneous micropores. The sample prepared by hydrolysis with MeOH+H₂O that gives the lowest gelling rate has very rough surface and large pore size, as compared with other samples that have lots of small pores resulting in higher surface area. The sample prepared by hydrolysis with MgO+H₂O has some MgO precipitated on the surface, but the quantity is very small. *Figure 4.16* are SEM micrographs of the same samples at magnification of 2000.



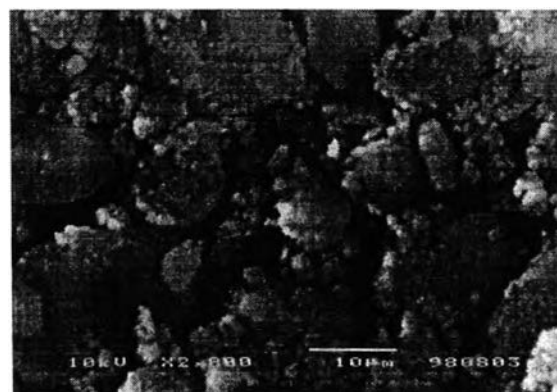
MeOH+H₂O x 2000



H₂O x 2000



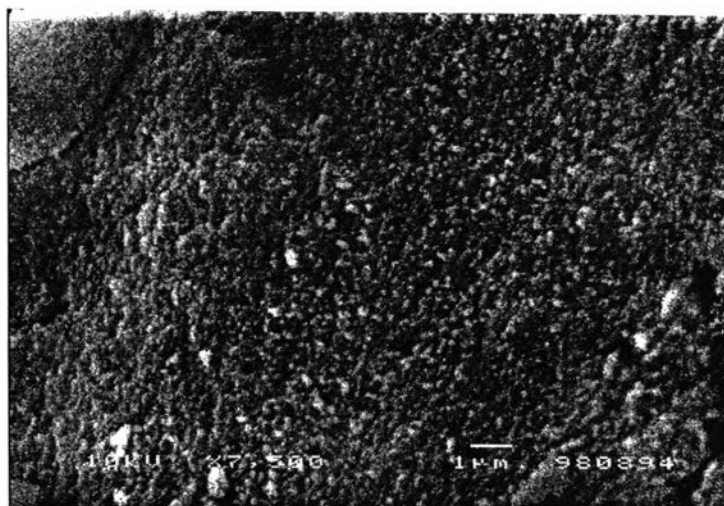
MgO+H₂O x 2000



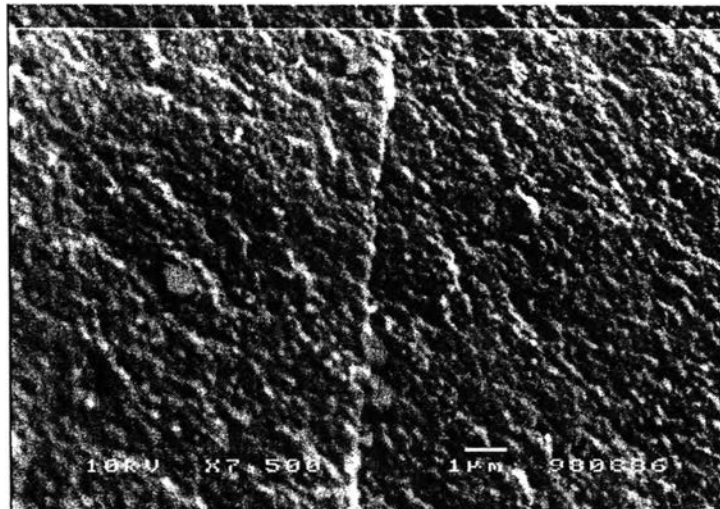
Fumed SiO₂ x 2000

Figure 4.16 SEM micrographs of pyrolyzed polysilatrane hydrolyzed with various solvents, at 800°C, and heating rate of 10°C/min as compared with fumed SiO₂, with magnification of 2000.

The other effect that is studied is the pyrolysis condition, as showed in the *Figure 4.17*.



Starting to pyrolyze at 500°C



Starting to pyrolyze at room temperature

Figure 4.17 SEM micrographs of pyrolyzed polysilatrane surface at different pyrolysis conditions.

From *Figure4.16* with magnification of 7500, it is seen clearly that the sample that is started to be pyrolyzed at 500°C has more pores inside, as compared with the one that started at room temperature.

We can summarize that the surface area, and porosity of the pyrolyzed sample are directly affected by the gelling rate and the pyrolysis condition. Moreover, the use of MgO to accelerate hydrolysis is resulted in some impurity in the products.

